consistent with the deuterium scrambling and isotope effects reported by Groves et al.[36] Although this matter is not completely settled, our results are in agreement with the mechanism proposed by Groves[37] for cyclohexene oxidation.

Synthetic Applications. We have not discussed here the use of pyrrole-halogenated metalloporphyrins such as octabromo-octachlorohemin.[26] Being more electronegative than any of those discussed here, these types of metalloporphyrins further extend the selectivity for epoxidation, show mechanisms that are more ET limiting, and are more resistant to destruction than any of those discussed here. We can therefore select metalloporphyrin catalysts to obtain desired products. For example, to epoxidize cyclohexene and similar alkenes, we would use the most electronegative iron(III) porphyrin available (Table I). To obtain cyclohexen-3-ol, we would use the most electropositive chromium porphyrin and carry the reaction to low conversion. At high conversion under these conditions almost pure cyclohexen-3-one would be obtained.

To obtain pure *exo*-norbornene epoxide, the (TPP)Cr(III) catalyzed reaction (exo/endo > 1000) is preferable even to MCPBA epoxidation (exo/endo = 690). On the other hand, we can obtain 20% *endo*-epoxide with the most electronegative iron porphyrins or electronegative *N*-alkyliron porphyrins. Although a separation is required, this one-step, high overall yield process is the easiest route to this epoxide.

As we have previously indicated,[32] the electronegative iron porphyrins also provide high selectivity for dienes over monoenes and for *cis*-alkenes over *trans*-alkenes. We also see little loss of stereospecificity with electronegative iron porphyrins whereas other iron porphyrins and manganese porphyrin catalyzed epoxidations give some loss of stereospecificity.

A comparison of kinetic properties of these metalloporphyrins that further delineates their differences will be reported elsewhere.

Acknowledgment. We are grateful to Professor R. S. Brown for a gift of adamantylideneadamantane and to the National Science Foundation (Grant CHE 87-21364) for financial support.

(36) Groves, J. T.; Avaria-Neisser, G. E.; Fish, K. M.; Imachi, M.; Kuczkowski, R. L. *J. Am. Chem. Soc.* **1986**, *108*, 3837.
(37) Groves, J. T.; Subramanian, D. V. *J. Am. Chem. Soc.* **1984**, *106*, 2177.

Intramolecular Energy Transfer in a Chromophore–Quencher Complex

Stephen Boyde, Geoffroy F. Strouse, Wayne E. Jones, Jr., and Thomas J. Meyer*

Contribution from the Department of Chemistry, University of North Carolina, Chapel Hill, North Carolina 27514. *Received December 27, 1988*

Abstract: Metal-to-ligand charge-transfer excitation of the complex $[Ru(bpyCH_2OCH_2An)_3]^{2+}$ ($bpyCH_2OCH_2An$ is 4-[(9-anthrylmethoxy)methyl]-4′-methyl-2,2′-bipyridine is followed by rapid (<5 ns), efficient intramolecular energy transfer to one of the chemically attached anthryl groups, to give the anthryl triplet, $-^3An$. It has a lifetime of 6 μs in CH_3CN at 295 K. Oxidative quenching of $[(bpyCH_2OCH_2An)_2Ru^{II}(bpyCH_2OCH_2{}^3An)]^{2+*}$ by PQ^{2+} (PQ^{2+} is paraquat) occurs initially at $-^3An$ with k(295 K, CH_3CN) = 2.2×10^9 M^{-1} s^{-1}. The oxidative quenching step is followed by rapid intramolecular electron transfer to give $[(bpyCH_2OCH_2An)_2Ru^{III}(bpyCH_2OCH_2An)]^{3+}$.

Photoconversion processes based on the electron-transfer quenching of molecular excited states are well established.[1-5] In this area a considerable effort has been expended in the search for molecules that have suitable excited-state lifetime and electron-transfer properties. Among the most versatile examples are polypyridyl complexes such as $[Ru(bpy)_3]^{2+}$ (bpy is 2,2′-bipyridine) where the ground-state electronic configuration is $(d\pi)^6$ and the relevant excited states are metal-to-ligand charge transfer (MLCT) in character.[5-10] An example of a photoconversion sequence based on the oxidative quenching of $[Ru(bpy)_3]^{2+*}$ by PQ^{2+} (PQ^{2+} is 1,1′-dimethyl-4,4′-bipyridinium dication) is shown in Scheme I.[1b]

Scheme I

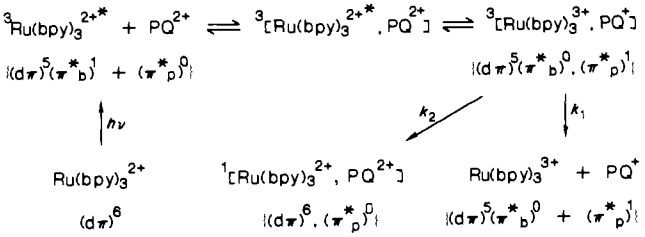

In the electronic configurations shown in Scheme I, π^*_b and π^*_p are the lowest lying π^* levels of bpy and PQ^{2+}. The dominant

(1) (a) Gafney, H. D.; Adamson, A. W. *J. Am. Chem. Soc.* **1972**, *94*, 8238. (b) Bock, C. R.; Meyer, T. J.; Whitten, D. F. *J. Am. Chem. Soc.* **1974**, *96*, 4710.
(2) (a) *Photochemical Conversion and Storage of Chemical Energy*; Connolly, J. S., Ed.; Academic Press: New York, 1981. (b) *Energy Resources Through Photochemistry and Catalysis*; Grätzel, M., Ed.; Academic Press: New York, 1983. (c) Bolton, J. S. *Science* **1978**, *202*, 705.
(3) (a) Sutin, N.; Creutz, C. *Pure Appl. Chem.* **1980**, *52*, 2717. (b) Sutin, N. *J. Photochem.* **1979**, *10*, 19.
(4) (a) Kirch, M.; Lehn, J.-M.; Sauvage, J.-P. *Helv. Chim. Acta* **1979**, *62*, 1345. (b) Darwent, J. R.; Douglas, P.; Harriman, A. *Coord. Chem. Rev.* **1982**, *44*, 83.
(5) (a) Kalyanasundaram, K. *Coord. Chem. Rev.* **1982**, *46*, 159. (b) Meyer, T. J. *Prog. Inorg. Chem.* **1983**, *30*, 389-440. (c) Juris, A.; Barigelletti, ; Campagna, S.; Balzani, V.; Belser, P.; Von Zelewsky, A. *Coord. Chem. Rev.* **1988**, *84*, 85-277.
(6) (a) Watts, R. J. *J. Chem. Educ.* **1983**, *60*, 834. (b) Seddon, E. A.; Seddon, K. R. *The Chemistry of Ruthenium*; Elsevier: Amsterdam, 1984; pp 1173-1316.
(7) (a) Hager, G. D.; Crosby, G. A. *J. Am. Chem. Soc.* **1975**, *97*, 7031. (b) Lacky, D. E.; Pankuch, B. J.; Crosby, G. A. *J. Phys. Chem.* **1980**, *84*, 2068. (c) Allsopp, S. R.; Cox, A.; Kemp, T. J.; Reed, W. J. *J. Chem. Soc., Faraday Trans.* **1974**, *96*, 629.
(8) (a) Ferguson, J.; Herren, F.; Krausz, E. R.; Vrbanich, J. *Coord. Chem. Rev.* **1985**, *64*, 21. (b) Yersin, H.; Gallhuber, E. *J. Am. Chem. Soc.* **1984**, *106*, 6582.
(9) Meyer, T. J. *Pure Appl. Chem.* **1986**, *50*, 1293.
(10) (a) Krause, R. A. *Struct. Bonding* **1987**, *67*, 1-52. (b) Krausz, E. R. *Comm. Inorg. Chem.* **1988**, *7*, 139.

0002-7863/89/1511-7448$01.50/0

spin character of the states involved is indicated by the spin multiplicities shown as superscripts to the left in the molecular formula.

MLCT excited states offer several advantages in such schemes:[1-10]

(i) Typically, they are chemically stable both in the excited state and in adjacent oxidation states. As a result, they can retain their chemical identities through an extended series of photocatalytic cycles.

(ii) They have intense absorption bands in the visible, and their absorption properties can be varied systematically by varying the ligands.

(iii) Although their underlying electronic structures are quite complex, the excited states are kinetically well behaved in electron-transfer reactions.

(iv) The existence of significant spin–orbit coupling at the metal causes low-lying singlet and triplet MLCT states to mix. Thus, intersystem crossing from the spectroscopically accessible excited states to the lowest states, which are largely triplet in character, occurs with high efficiency.

The last of these properties is a two-edged sword. Singlet–triplet mixing may enhance intersystem crossing, but it also lifts the spin restriction to excited-state decay. As a result, the excited-state lifetime for $[Ru(bpy)_3]^{2+*}$ at room temperature is on the order of 1 μs, which is short compared to the lifetimes of typical organic triplets.[11] With the decrease in lifetime a relatively high concentration of quencher is required if diffusional quenching is to compete with excited-state decay.

Another, more subtle effect of singlet–triplet mixing occurs in the back-electron-transfer step in Scheme I (k_2). There is a spin prohibition to back electron transfer because of the spin change that occurs between triplet and singlet states.[12] However, for the $(d\pi)^5$ electronic configuration in $[Ru(bpy)_3]^{3+}$, the spin prohibition is lifted by spin–orbit coupling at Ru^{III} which induces singlet–triplet mixing.[13] With singlet–triplet mixing the rate constant for back electron transfer is enhanced. As a result, in the $[Ru(bpy)_3]^{2+}/PQ^{2+}$ system in Scheme I, only 15–20% of the redox products produced in the quenching step actually escape from the solvent cage.[14] Back electron transfer is more rapid and limits the appearance of separated redox products.

By contrast, photoconversion based on the triplet states of organic chromophores like anthracene take advantage of longer lifetimes and the spin prohibition to back electron transfer to achieve high quantum yields for cage escape at low quencher concentrations.[15-21] However, organic sensitizers are prone to photodecomposition and their radical cations and anions tend to be unstable. Furthermore, they typically absorb light appreciably only at relatively high energies in the near UV. The singlet excited states that result from UV excitation are short lived and typically undergo intersystem crossing to the lower lying triplet with less than unit efficiency.

The limitations inherent in the separate organic and metal complex systems have been circumvented by including both types of chromophore in the same solution based system. Thus, visible excitation of $[Ru(bpy)_3]^{2+}$ in the presence of anthracene (An) or some of its derivatives leads to ^3An, by energy transfer, with near unit efficiency.[18-21] Once formed, ^3An can be oxidatively quenched by PQ^{2+} to give An^+ and PQ^+ in high yield. The $Ru(bpy)_3^{2+}/An/PQ^{2+}$ system has been exploited to achieve high efficiencies for hydrogen evolution[20] and has been extended to more complex systems based on redox quenchers attached to soluble polymers.[22] One limitation is that a considerable excess of anthracene is required for the bimolecular quenching of the MLCT excited state.

We describe here the preparation of a metal complex–quencher assembly that combines the desirable features of both the MLCT and anthryl $\pi-\pi^*$ excited states in a single molecule. The intramolecular system offers the advantages of visible light absorptivity, stability, and enhanced efficiencies, without the requirement for bimolecular quenching. Our approach has been based on the synthesis of an anthryl-containing derivative of 2,2′-bipyridine. The compound is 4-[(9-anthrylmethoxy)-methyl]-4′-methyl-2,2′-bipyridine ($bpyCH_2OCH_2An$). We have

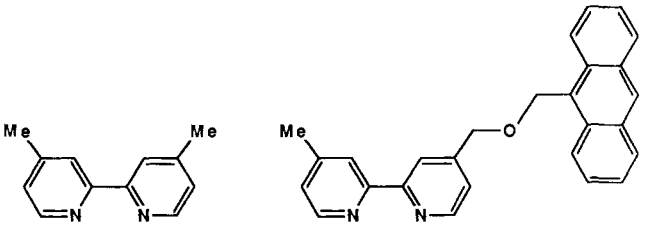

dmb $bpyCH_2OCH_2An$

used the ligand to prepare the chromophore–quencher complex $[Ru(bpyCH_2OCH_2An)_3]^{2+}$ and report here a comparison of its photophysical and photochemical properties with those of the model complex $[Ru(dmb)_3]^{2+}$ (dmb is 4,4′-dimethyl-2,2′-bipyridine).

Experimental Section

Materials and Methods. The complexes $[Ru(dmso)_4Cl_2]$,[23] $[Ru(dmb)_3][PF_6]_2$,[24,25] and 4-bromomethyl-4′-methylbipyridine[26] were prepared by established procedures. The compound 9-anthracenemethanol was obtained from Aldrich and used as supplied. All solvents used in preparations were reagent grade and were used as supplied except where specified. Spectrophotometric grade acetonitrile (Burdick and Jackson) was used for all spectroscopic and electrochemical measurements. Chemical analyses were performed by Galbraith Labs (Knoxville, TN). Syntheses and sample preparations were carried out in the dark under an inert atmosphere where possible.

Instrumentation and Measurements. UV–visible spectra were recorded on solutions contained in 1-cm path length cuvettes, on a Hewlett-Packard 8451A diode array spectrophotometer or on a Cary 14 dual-beam scanning instrument. ^1H NMR spectra were recorded on a Varian XL-400 400-MHz spectrometer. Emission spectra were recorded on a Spex Fluorolog-2 emission spectrophotometer equipped with a 450-W xenon lamp and a cooled Hamamatsu R928 photomultiplier tube and were corrected for instrument response.

Time-resolved emission measurements were made by using a PRA LN1000/LN102 nitrogen laser/dye laser combination for sample excitation. Emission was monitored at a right angle to the excitation source by using a PRA B204-3 monochromator and a cooled, 10-stage, Hamamatsu R928 PMT, coupled to a LeCroy 9400 digital oscilloscope interfaced to an IBM PC. Solution concentrations of ca. 1×10^{-5} M in a cuvette of 1-cm path length were utilized after Ar bubble or freeze–pump–thaw degassing to purge oxygen from the cuvette.

Transient absorbance measurements were performed by using a Quanta Ray DCR-2A Nd:YAG laser pumping coumarin 460 in a PDL-2 dye laser to produce an excitation pulse of ca. 6 ns at <4 mJ/pulse. The

(11) (a) Birks, J. B. *Photophysics of Aromatic Molecules*; Wiley: London, 1970. (b) Turro, N. J. *Molecular Photochemistry*; W. A. Benjamin: New York, 1967.
(12) (a) Wigner, E. *Z. Phys.* **1927**, *40*, 492, 883. (b) Gouterman, M.; Holten, P. *Photochem. Photobiol.* **1977**, *25*, 85.
(13) Olmsted, J., III; Meyer, T. J. *J. Phys. Chem.* **1987**, *91*, 1649.
(14) Hoffman, M. Z. *J. Phys. Chem.* **1988**, *92*, 3458, and references therein.
(15) Chan, M. S.; Bolton, J. R. *Photochem. Photobiol.* **1981**, *34*, 537.
(16) Kalyanasundaram, K.; Dung, D. *J. Phys. Chem.* **1980**, *84*, 2551.
(17) Davidson, R. S.; Bonneau, R.; Fornier de Violet, P.; Joussot-Dubien, J. *Chem. Phys. Lett.* **1981**, *78*, 475.
(18) Mau, A. W.-H.; Johansen, O.; Sasse, W. H. F. *Photochem. Photobiol.* **1985**, *41*, 503.
(19) Johansen, O.; Mau, A. W.-H.; Sasse, W. H. F. *Chem. Phys. Lett.* **1983**, *94*, 107.
(20) Johansen, O.; Mau, A. W.-H.; Sasse, W. H. F. *Chem. Phys. Lett.* **1983**, *94*, 113.
(21) Wrighton, M.; Markham, J. *J. Phys. Chem.* **1973**, *77*, 3042.
(22) Olmsted, J., III; McClanahan, S. F.; Danielson, E.; Younathan, J. N.; Meyer, T. J. *J. Am. Chem. Soc.* **1987**, *109*, 3297.
(23) Evans, I. P.; Spencer, A.; Wilkinson, G. *J. Chem. Soc., Dalton Trans.* **1973**, 204.
(24) Wacholtz, W. A.; Auerbach, R. A.; Schmehl, R. H. *Inorg. Chem.* **1986**, *25*, 227.
(25) Wacholtz, W. A.; Auerbach, R. A.; Schmehl, R. H. *Inorg. Chem.* **1987**, *26*, 2986.
(26) Boyde, S.; Strouse, G. F.; Jones, W. E.; Meyer, T. J., unpublished results.

excitation beam was coincident to an Applied Photophysics Limited laser kinetic spectrometer. It included a 250-W pulsed Xe arc probe source, quartz optics, a $f/3.4$ grating monochromator, and a five-stage PMT. The output was coupled to a LeCroy 9400 digital oscilloscope interfaced to an IBM PC. Electronic control and synchronization of laser, probe, and digital oscilloscope was provided by electronics of our own design. A 400-nm cutoff filter was used to prevent direct probe beam excitation of anthracene. Full spectrum transient absorbance measurements were made on solutions containing the complex at 5×10^{-5} M which had been freeze–pump–thaw degassed in a tipsy cell. The tipsy cell, which was of home design, allowed for the replacement of old solution by fresh solution in the sealed environment of the cell. Old solution was replaced by fresh solution after every three or four points in the spectrum had been acquired.

In the quenching experiments, transient absorbance measurements were carried out on solutions containing $[Ru(bpyCH_2OCH_2An)_3]^{2+}$ or $[Ru(dmb)_3]^{2+}$ in MeCN/0.1 M $[N(n\text{-}Bu)_4][PF_6]$ in the presence of 10 mM $[PQ][PF_6]_2$. To allow for a direct comparison of results obtained for the two complexes, their concentrations were adjusted to 5×10^{-5} M to give an absorbance at the pump wavelength, 460 nm, of 0.70 ± 0.01.

The solutions were bubble degassed with Ar, in a cuvette with a 1-cm path length, to purge O_2 from the system. The quantity of PQ^+ produced was determined by monitoring the absorbance difference that appeared at 610 nm following 460-nm excitation. The ion PQ^+ has a molar extinction coefficient of approximately 1.3×10^4 M^{-1} cm^{-1} at 610 nm.[27,28] None of the other components of the mixture absorb significantly at this wavelength. There was some interference due to emission from the complexes. The emission was subtracted from the transient signal before calculating the absorbance changes.

HPLC was carried out on a Perkin-Elmer Series 4 liquid chromatograph with an LC-94 UV–vis detector by using conditions described elsewhere.[31] For the decomposition experiments a Whatman CN-PAK column was utilized, and the sample was eluted with a 9:1 mixture of CH_2Cl_2:MeOH with 1% $[N(n\text{-}Bu)_4][PF_6]$ added.

Synthesis. Preparation of $bpyCH_2OCH_2An$.[29] Powdered KOH (0.085 g, 1.52 mmol) was added to dry DMSO (2 mL) and stirred for 5 min. The compound 9-anthracenemethanol (0.079 g, 0.38 mmol) was added, the solution was stirred for 10 min, and 4-bromomethyl-4′-methylbipyridine (0.2 g, 0.76 mmol) was added. The solution was stirred at room temperature under Ar for 15 h and added to H_2O (10 mL). The mixture was extracted with CH_2Cl_2 (3×10 mL), and the combined organic extracts were dried over $MgSO_4$ and evaporated to dryness. The residue was purified by column chromatography on silica (Aldrich, 70-230 mesh), and eluted with EtOAc/hexane. The desired product, which was readily identifiable by its intense blue fluorescence under 366-nm excitation and by the appearance of a dark red color when the solution was spotted on a $FeSO_4$ soaked TLC plate, eluted as the first band. The yield after recrystallization from ether was 40%.

Anal. Calcd for $C_{27}H_{22}N_2O$: C, 83.05; H, 5.67; N, 7.17. Found: C, 82.23; H, 5.89; N, 6.55. UV–vis (CH_2Cl_2) (λ_{max} (nm) (ϵ in M^{-1} cm^{-1})) 258 (91 200), 284 (18 800), 334 (4100), 350 (5900), 368 (6900), 388 (6100). ^1H NMR (ppm vs. TMS) δ 2.46 (3 H, s, $-CH_3$), 4.80 (2 H, s, bpy-CH_2-), 5.55 (2 H, s, An-CH_2-), (7.1, 1 H, d), 7.32 (1 H, d), 7.5 (4 H, m), 7.97 (2 H, d), 8.2 (1 H, s), 8.37 (1 H, s), 8.35 (2 H, d), 8.45 (1 H, s), 8.53 (1 H, d), 8.65 (1 H, d).

Preparation of $[Ru(bpyCH_2OCH_2An)_3][PF_6]_2$. $[Ru(dmso)_4Cl_2]$ (0.107 g, 0.22 mmol) was dissolved in ethylene glycol (30 mL) and brought to reflux for 5 min. The flask was transferred to a 120 °C oil bath and stirred as $bpyCH_2OCH_2An$ (0.25 g, 0.64 mmol) was added. The solution was stirred under Ar, protected from light, for 3 h, cooled to room temperature, and added to aqueous $K[PF_6]$ (50 mL, 0.5 M). The powdery red precipitate was collected by centrifugation and washed with H_2O (2×10 mL), dried under vacuum, and reprecipitated from $MeCN/Et_2O$. The yield was 78%.

Anal. Calcd for $C_{81}H_{66}N_{12}O_3RuP_2F_{12}$: C, 62.3; H, 4.25; N, 5.38. Found: C, 62.2; H, 4.24; N, 5.38.

Purification of $[Ru(bpyCH_2OCH_2An)_3][PF_6]_2$. The ether link that bonds the anthryl and bpy groups in $bpyCH_2OCH_2An$ is subject to slow solvolysis in polar organic solvents because of the reactivity of 9-methylanthryl as a leaving group.[30] This leads to slow decomposition of $[Ru(bpyCH_2OCH_2An)_3]^{2+}$ and to the appearance of emitting impurities. The PF_6^- salt of the complex was purified by column chromatography on neutral alumina (Fisher, 80-200 mesh) with 1:1 MeCN/toluene as the eluent. The purity of solutions containing the complex was conveniently checked by TLC, either on alumina eluted with 1:1 MeCN/toluene or on silica eluted with 0.1 M $[N(n\text{-}Bu)_4][PF_6]$/MeCN. In both media the pure complex was the only species observed in freshly chromatographed solutions. It appeared as a well-defined spot with a R_f of 0.8–0.95, which did not luminesce detectably under long-wavelength UV excitation. In aged solutions that were many hours old, several other spots with much lower R_f values (0.0–0.1) were also present. These spots were typically too faint to be detectable visibly but were strongly luminescent under UV light.

The light sensitivity of the complex in CH_3CN was investigated by HPLC. Under normal transient absorbance experimental conditions (see above) there was negligible decomposition over a 3-h period. Thus, the complex was stable over the period of time necessary to run the experiments. UV-induced decomposition was avoided in transient absorbance experiments by placing a 400-nm cutoff filter in front of the Xe lamp probe source.

When pure solutions containing $[Ru(bpyCH_2OCH_2An)_3][PF_6]_2$ were chromatographed on silica TLC plates with a lower polarity eluent (e.g., 0.01 M $[N(n\text{-}Bu)_4][PF_6]$ in 1:1 MeCN/toluene), the spot due to the complex could be resolved into two very closely spaced, crescent-shaped bands. We believe that these bands are due to the fac and mer isomers of $[Ru(bpyCH_2OCH_2An)_3]^{2+}$. We have been unable to separate them or even to alter their relative concentrations, either by fractional crystallisation or by preparative chromatography.

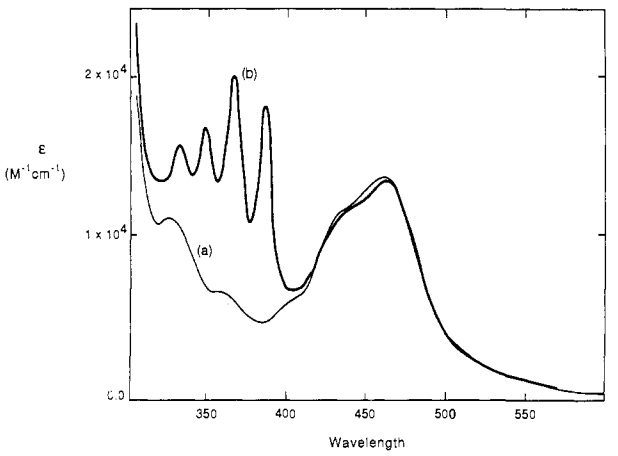

Figure 1. Absorption spectra of (a) $Ru(dmb)_3^{2+}$ and (b) $Ru(bpyCH_2OCH_2An)_3^{2+}$, in acetonitrile at room temperature.

Table I. Spectral and Lifetime Data in Acetonitrile at Room Temperature

complex	λ_{max}^{abs},[a] nm	λ_{max}^{em}, nm	φ_{em}[b]	τ, ns
$Ru(dmb)_3^{2+}$	461	642	9×10^{-2}	950
$Ru(bpyCH_2OCH_2An)_3^{2+}$	462	654[c]	2×10^{-4}	<5[c]

[a] λ_{max} for the lowest energy, high-absorptivity, MLCT transition. [b] Emission quantum yield, excitation at 460 nm. [c] Emission is from the MLCT state. The anthryl triplet state, which is formed by intramolecular sensitization (see text) does not contribute to the emission. It has a lifetime of 15 ± 1 μs.

Results

Absorption and Emission Spectra. The UV–visible spectra of $[Ru(bpyCH_2OCH_2An)_3]^{2+}$ and $[Ru(dmb)_3]^{2+}$ are illustrated in Figure 1. Absorption and emission maxima, as well as excited-state lifetimes obtained by emission decay, are collected in Table I. The intense absorption features in the visible arise from $d\pi(Ru) \rightarrow \pi^*(bpy)$ MLCT transitions.[6-10] By comparing spectral profiles, it is clear that the patterns and energies of the MLCT transitions at longer wavelengths are essentially unperturbed by the anthryl substituents on the ligands. The narrow, structured absorption bands in the near UV also appear for $bpyCH_2OCH_2An$ and arise from anthracene-localized $\pi \rightarrow \pi^*$ transitions.[11]

The emission spectrum of $[Ru(bpyCH_2OCH_2An)_3]^{2+}$ (Figure 2) obtained in CH_3CN at 295 K with 460-nm excitation is very similar in profile to that of $[Ru(dmb)_3]^{2+}$ although it is slightly red shifted and broadened.[24,25] The spectral similarities in emission and absorption spectra show that $[Ru(dmb)_3]^{2+}$ provides a good

(27) Watanabe, T.; Honda, K. *J. Phys. Chem.* **1982**, *86*, 2617.
(28) Rougee, M.; Ebbesen, T.; Shetti, F.; Bensasson, R. V. *J. Phys. Chem.* **1982**, *86*, 4404.
(29) Johnstone, R. A. W.; Rose, M. E. *Tetrahedron* **1979**, *35*, 2169.
(30) Jaeger, C. W.; Kornblum, N. *J. Am. Chem. Soc.* **1972**, *94*, 2545.
(31) Boyde, S.; Strouse, G. F.; Meyer, T. J., manuscript in preparation.

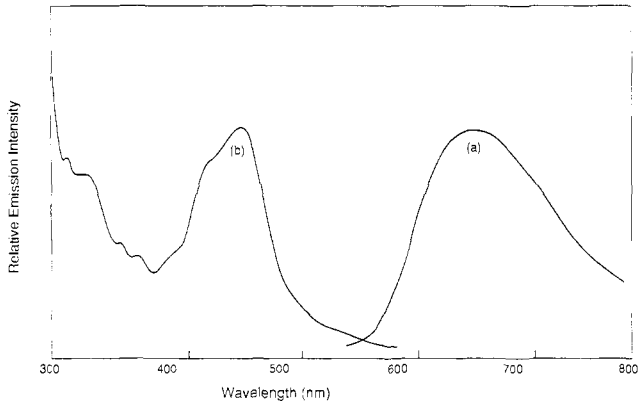

Figure 2. Emission spectrum (a), excitation at 460 nm, and excitation spectrum (b), monitored at 650 nm, of $Ru(bpyCH_2OCH_2An)_3^{2+}$ in acetonitrile at room temperature.

model for the underlying MLCT electronic structure in $[Ru(bpyCH_2OCH_2An)_3]^{2+}$. The excitation spectrum in Figure 2 is essentially an overlay of the absorption spectrum except that excitation in the anthracene $\pi \rightarrow \pi^*$ region below 400 nm does not lead to appreciable emission. Emission from $[Ru(bpyCH_2OCH_2An)_3]^{2+}$ is of low intensity with a quantum yield ca. 2% that of $[Ru(dmb)_3]^{2+}$ (Table I).[32a]

The free $bpyCH_2OCH_2An$ ligand exhibits an intense, structured fluorescence under UV excitation, with emission maxima at 400, 421, 442, and 464 nm in CH_2Cl_2 solution with 385-nm excitation. By comparing the integrated emission intensity for anthracene in benzene under the same instrumental conditions, we estimate that the fluorescence quantum yield for $bpyCH_2OCH_2An$ is 0.3.[32b] By contrast, excitation of $[Ru(bpyCH_2OCH_2An)_3]^{2+}$ at 385 nm leads to a weaker emission with resolvable components at 420 and 440 nm. This emission is even weaker, $\phi_{em} < 2 \times 10^{-4}$, than the low-energy MLCT emission.

Time-Resolved Measurements. Time-resolved emission measurements following 460-nm excitation show that the lifetime for MLCT emission from $[Ru(bpyCH_2OCH_2An)_3]^{2+}$ is too short (<5 ns) to be measured with our instrumentation, either in CH_3CN solution at room temperature (295 ± 1 K) or in a 5:2 EtOH/DMF glass at 100 K. The MLCT emission lifetime for $[Ru(dmb)_3]^{2+}$ in CH_3CN is 950 ns, which is in reasonable agreement with the literature value.[24,25] The greatly decreased emission lifetime for $[Ru(bpyCH_2OCH_2An)_3]^{2+}$ shows that once it is formed, the MLCT excited state must be rapidly quenched.

A transient absorbance difference spectrum for $[Ru(bpyCH_2OCH_2An)_3]^{2+}$ obtained 1 μs after 460-nm excitation in CH_3CN at room temperature is shown in Figure 3. The difference spectrum for $[Ru(dmb)_3]^{2+}$ obtained under the same conditions but 50 ns after the laser pulse is shown for comparison. In agreement with other MLCT excited states,[33-35] the spectrum of $[Ru(dmb)_3]^{2+*}$ consists of $\pi \rightarrow \pi^*$ absorption features at ca. 385 and 550 nm and a bleach in the 450-nm region due to the loss in ground-state MLCT absorption. The decay of the excited state follows simple first-order kinetics throughout the near UV and visible with the same 950-ns lifetime observed by emission decay.

The transient absorbance difference spectrum of the chromophore–quencher complex has a single feature. Following excitation at 460 nm, an excited state is formed that has an intense absorbance maximum at 430 nm and decays by single-exponential kinetics with $\tau = 5.9 \pm 0.6$ μs. The absorbance maximum of the

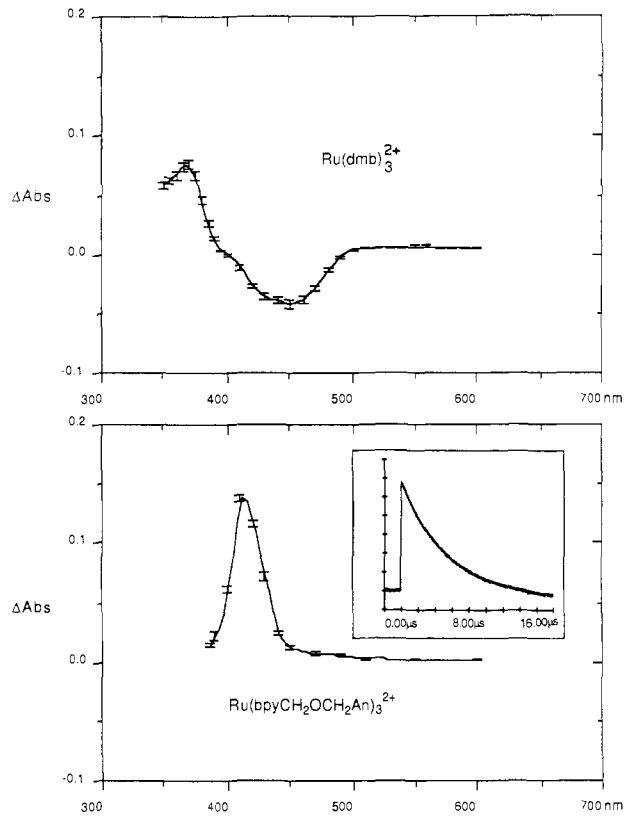

Figure 3. Transient absorbance difference spectra obtained following 460-nm excitation in CH_3CN at room temperature. The spectrum of $Ru(dmb)_3^{2+}$ was acquired 50 ns after the laser pulse, and the spectrum of $[Ru(bpyCH_2OCH_2An)_3]^{2+*}$ 1 μs after the pulse. The transient absorbance decay for $[Ru(bpyCH_2OCH_2An)_3]^{2+*}$, monitored at 430 nm, is shown in the inset (τ = 15 μs).

excited state coincides with λ_{max} for the lowest triplet state of anthracene,[21,36] showing that MLCT excitation leads to intramolecular sensitization of the bound anthryl triplet, $-^3An$. Direct excitation into the anthryl portion of the complex at 355 nm also results in efficient formation of $-^3An$ as shown by the appearance of its characteristic 430-nm absorbance in the difference spectrum. The 430-nm absorbance appears within the duration of the laser pulse (ca. 5 ns) following excitation at either wavelength. There is no evidence in the transient spectra for absorbance features attributable to the MLCT excited state. The same absorbance maximum for $-^3An$ was observed in a frozen 5:2 EtOH/DMF solution at 100 K following MLCT excitation. Under these conditions the lifetime of the anthryl triplet is extended to >100 μs.

There are two sets of positional isomers for $[Ru(bpyCH_2OCH_2An)_3]^{2+}$ arising from the asymmetry at the 4,4′ positions of the ligands. In the facial isomers, the $-CH_2OCH_2An$ groups are mutually cis. In the meridional isomers one $-CH_2OCH_2An$ group is cis to a second and trans to a third. As noted in the Experimental Section, there is HPLC evidence for the presence of both types of isomers in our samples. Their photophysical properties must be very similar. This is shown, for example, by the fact that in samples that appear to be mixtures of the two isomers, decay of $-^3An$ is by simple first-order kinetics.

Oxidative Quenching. In Figure 4 are shown transient absorbance traces recorded at 610 nm following 460-nm excitation of solutions containing $[Ru(dmb)_3]^{2+}$ or $[Ru(bpyCH_2OCH_2An)_3]^{2+}$ and 1×10^{-2} M PQ^{2+}. In either case the growth in absorbance at the maximum for PQ^+ at 610 nm shows that oxidative quenching occurs following laser excitation. The rate constant

(32) (a) The emission quantum yield for $[Ru(dmb)_3]^{2+}$ in MeCN was measured relative to the same complex in CH_2Cl_2, for which $\phi_{em} = 0.12$.[24] (b) ϕ_{em} for anthracene in benzene is ca. 0.25, from ref 11b, Table 4.5.

(33) Creutz, C.; Chou, M.; Netzel, T. L.; Okumura, M.; Sutin, N. *J. Am. Chem. Soc.* **1980**, *102*, 1309.

(34) Bensasson, R.; Salet, C.; Balzani, V. *J. Am. Chem. Soc.* **1976**, *98*, 3722.

(35) Lachish, U.; Infelta, P. P.; Grätzel, M. *Chem. Phys. Lett.* **1979**, *62*, 317.

(36) (a) Reference 11a, Table 6.11, p 280; Table 6.3, p 256. Reference 11b, Table 4-12, p 70. (b) Porter, G.; Windsor, M. W. *Proc. R. Soc. A* **1958**, *245*, 238. (c) McGlynn, S. P.; Boggus, J. D.; Elder, E. *J. Chem. Phys.* **1960**, *32*, 357.

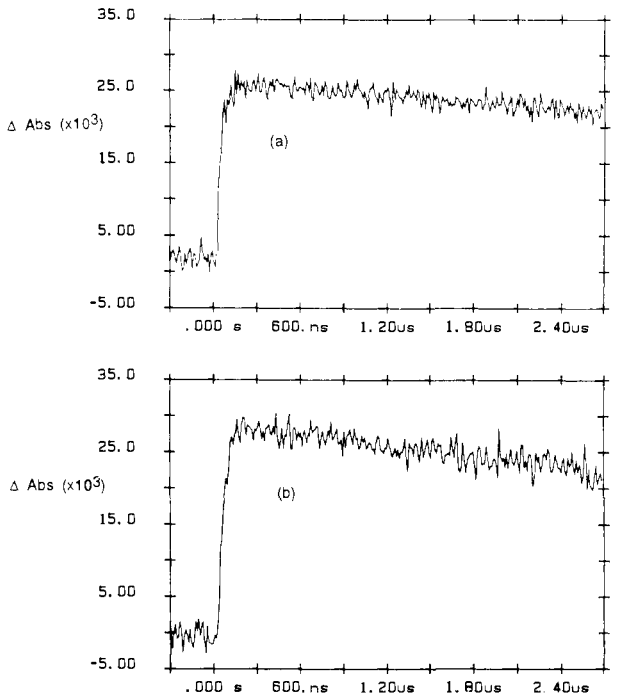

Figure 4. Absorbance vs time traces at 610 nm following 460-nm excitation of (a) $Ru(dmb)_3^{2+}$ or (b) $Ru(bpyCH_2OCH_2An)_3^{2+}$ with 10 mM PQ^{2+} in CH_3CN at 295 K.

for the oxidative quenching of $[Ru(dmb)_3]^{2+*}$ by PQ^{2+}, $k_q = 1.5 \times 10^9\ M^{-1}\ s^{-1}$, was determined by emission quenching by using standard Stern–Volmer techniques. For the quenching of $[Ru(bpyCH_2OCH_2An)_3]^{2+*}$, $k_q = 2.2 \times 10^9\ M^{-1}\ s^{-1}$. This rate constant was determined by observing the growth of PQ^+ by transient absorbance, Figure 4a, because of the very weak emission from the complex.

As shown in the absorbance vs time traces in Figure 4, the absorbance at 610 nm increases rapidly as quenching proceeds, reaching a maximum at $t = 100$ ns at which point quenching is virtually complete. Past 100 ns there is a loss in absorbance at both wavelengths due to diffusional back electron transfer between Ru^{III} and PQ^+. By analyzing the traces in this time domain according to second-order, equal-concentration kinetics, the back-electron-transfer rate constants are $\sim 1 \times 10^{10}\ M^{-1}\ s^{-1}$ for both $[Ru(dmb)_3]^{3+}$ and $[Ru(bpyCH_2OCH_2An)_3]^{3+}$. For both complexes, the maximum value of the absorbance change at 610 nm was $(25 \pm 5) \times 10^{-3}$, which corresponds to a maximum PQ^+ concentration of 3.3×10^{-6} M.

Following oxidative quenching, PQ^+ and either $[Ru(dmb)_3]^{3+}$ or $[Ru(bpyCH_2OCH_2An)_3]^{3+}$ appear in solution by a series of reactions like those shown in Scheme I. The overall efficiency with which they appear is given by the product $\eta^*\eta_q\eta_{sep}$.[14] The constant η^* is the efficiency of formation of the excited state that is quenched, η_q is the efficiency of the quenching process, and η_{sep} is the efficiency of separation (cage escape). A value of η^* near unity has been observed for the emitting state of $[Ru(bpy)_3]^{2+*}$ throughout the visible and near UV.[37] At the concentration of PQ^{2+} used in the oxidative quenching experiments in Figure 4 (10 mM), η_q is >0.95 for both complexes. Under these conditions of nearly complete quenching, equal concentrations of PQ^+ and Ru(III) appear for either complex following laser flash photolysis. If η^* is the same for both complexes, their separation efficiencies following oxidative quenching must also be the same. There is no apparent gain in η_{sep} following oxidative quenching of $[Ru(bpyCH_2OCH_2An)_3]^{2+*}$ by PQ^{2+} when compared to $[Ru(dmb)_3]^{2+*}$.

The changes in transient absorbance that occur at 430 nm when a solution containing $[Ru(bpyCH_2OCH_2An)_3]^{2+}$ and 10 mM PQ^{2+} undergoes laser flash photolysis at 460 nm are shown in Figure

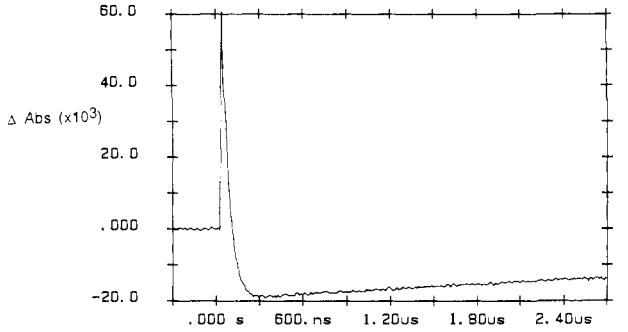

Figure 5. Absorbance vs time trace at 430 nm following 460-nm excitation of $Ru(bpyCH_2OCH_2An)_3^{2+}$ in CH_3CN with 10 mM of added PQ^{2+} at 295 K.

Scheme II

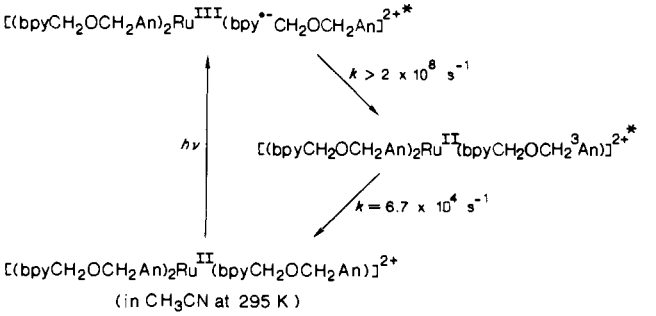

5. The initial absorbance due to $-^3$An is rapidly bleached on the same time scale that PQ^+ appears at 610 nm. The bleach returns to the base line on the same, slower time scale as the disappearance of the PQ^+ absorbance at 610 nm.

Discussion

Intramolecular Energy Transfer. The greatly reduced lifetime and emission quantum yield for the MLCT excited state of $[Ru(bpyCH_2OCH_2An)_3]^{2+}$, relative to $[Ru(dmb)_3]^{2+}$, imply that an efficient intramolecular quenching process occurs in the anthryl-containing complex following MLCT excitation. The appearance of the characteristic $-^3$An triplet absorption at 430 nm demonstrates that the quenching mechanism is by triplet energy transfer to anthracene (Scheme II). The decrease in emission quantum yield to 2% of that for $[Ru(dmb)_3]^{2+*}$ and the appearance of the intense $-^3$An triplet–triplet absorption feature at 430 nm show that the efficiency of energy transfer is near unity.

The dynamics of the quenching process were too rapid for us to resolve. The sub-5-ns lifetime for the residual MLCT emission is the basis for the lower limit of $2 \times 10^8\ s^{-1}$ for k_q cited in Scheme II. Measurements in a frozen 5:2 EtOH/DMF glass show that energy transfer continues to occur rapidly even at 100 K.

The energy of the lowest triplet excited state of anthracene is 14 900 cm^{-1},[36] and the energy of the MLCT excited state of $[Ru(dmb)_3]^{2+}$ is 16 850 cm^{-1}.[24,25] By using these values as estimates for the energies of the MLCT and $-^3$An excited states in $[Ru(bpyCH_2OCH_2An)_3]^{2+}$, the intramolecular energy-transfer process in Scheme II is exothermic by approximately 2000 cm^{-1} (0.25 eV). This represents a loss of 14% of the initial MLCT excited-state energy. Although excited-state energy is lost in the energy-transfer step, there is a compensating increase in excited-state lifetime of nearly an order of magnitude for $-^3$An (0.9 μs compared to 6 μs).

Photophysical Properties. We have been unable to detect phosphorescence from the $-^3$An excited state in $[Ru(bpyCH_2OCH_2An)_3]^{2+*}$. The lifetimes of this state in the free ligand and in $[Ru(bpyCH_2OCH_2An)_3]^{2+}$ are comparable.[26] By using the radiative rate constant of 0.5 s^{-1} for the anthracene triplet[38] and the lifetime of $-^3$An, it can be estimated that the

(37) Demas, J. N. *Inorg. Chem.* **1979**, *18*, 3177.

(38) Kasha, M. *J. Chem. Phys.* **1952**, *20*, 71.

phosphorescence quantum yield for ^{3}An is $\sim 3 \times 10^{-6}$. An emission at this level would be too weak to detect with our transient emission instrumentation and would be masked by the low-energy MLCT emission in the steady-state emission spectrum.

Compared to the free ligand, fluorescence from the singlet anthryl state of $[Ru(bpyCH_2OCH_2An)_3]^{2+}$ following direct UV excitation at 355 nm is decreased by $>10^3$. The results of the transient absorbance experiment following 355-nm excitation show that $\pi \rightarrow \pi^*$ singlet excitation leads to ^{3}An with high efficiency. A series of ^{1}MLCT and ^{3}MLCT states exist that lie between the ^{1}An and ^{3}An states. The existence of these states is shown by the MLCT absorption manifold in Figure 1 and follows from the results of analyses of the electronic structures of related complexes.[39,40] Although they exist, the intermediate MLCT states are *not* utilized appreciably in the interconversion between the ^{1}An and ^{3}An states. This is shown in the excitation spectrum in Figure 1 by the failure of $\pi \rightarrow \pi^*$ singlet excitation to lead to appreciable sensitization of the short-lived MLCT emission.

The loss of fluorescence in the complex must come from a greatly enhanced rate for ^{1}An $\rightarrow$ ^{3}An intersystem crossing by a direct process that bypasses the several intermediate MLCT states. The origin of the rate enhancement may lie in the adjacent Ru^{II} ion and its external heavy-atom effect. In this case, the heavy-atom effect could have its origin electronically in partial charge transfer from the $(d\pi)^6$ Ru^{II} ion to the hole in the $\pi \rightarrow \pi^*$ excited state. Partial charge transfer would lead to the mixing of MLCT character into ^{1}An with the introduction of the spin–orbit coupling character needed to enhance the ^{1}An $\rightarrow$ ^{3}An transition.

Intramolecular Oxidative Quenching. In addition to obtaining an extended excited-state lifetime following intramolecular energy transfer, we were interested in exploring the possibility that electron-transfer quenching of $[(bpyCH_2OCH_2An)_2Ru(bpyCH_2OCH_2{}^3An)]^{2+*}$ might proceed with the high efficiency for cage escape found for pure organic triplets.[18-20] The thought was that MLCT excitation and intramolecular energy transfer would lead to the anthryl triplet as in Scheme II. Following bimolecular quenching by PQ^{2+}, there would be a spin prohibition to back electron transfer between $-An^+$ and PQ^+ in the association complex because the oxidized site is $-An^+$ and not Ru^{III}:

$$^3[(bpyCH_2OCH_2An)_2Ru^{II}(bpyCH_2OCH_2An^+)^{3+}, PQ^+] \rightarrow {}^1[(bpyCH_2OCH_2An)_2Ru^{II}(bpyCH_2OCH_2An)^{2+}, PQ^{2+}]$$

With the spin prohibition, the rate of back electron transfer should be decreased and separation enhanced. This mechanism does appear to contribute to the enhanced separation efficiencies obtained for organic triplets compared, for example, to $[Ru(bpy)_3]^{2+*}$.[22]

The nearly identical separation efficiencies found for the quenching of $[Ru(dmb)_3]^{2+*}$ and $[Ru(bpyCH_2OCH_2An)_3]^{2+*}$ by PQ^{2+} indicate that the spin apparatus for reducing back-electron-transfer rates is lost in the anthryl-containing complex. The reason for this somewhat disappointing result is revealed by the spectral changes that occur for $[Ru(bpyCH_2OCH_2An)_3]^{2+}$ at 430 nm following laser excitation in the presence of added PQ^{2+} (Figure 5). At this wavelength, the initially strong absorbance due to ^{3}An is rapidly lost and converted into a bleach. The decrease in absorbance at 430 nm occurs on the same time scale as the appearance of PQ^+ at $\lambda_{max} = 610$ nm. The bleach arises from loss of the Ru^{II} MLCT chromophore in the PQ^{2+}-quenching step. It subsequently returns to the base line on the same time scale that PQ^+ is converted into PQ^{2+}. The only significant ground-state absorbance at this wavelength comes from the chromophore. The maximum absorbance loss in the bleaching region occurs at ca. 455 nm, which is a λ_{max} for the $d\pi \rightarrow \pi^*$(dmb) MLCT spectral manifold (Figure 1).

We conclude from these observations that the quenching of $[(bpyCH_2OCH_2An)_2Ru^{II}(bpyCH_2OCH_2{}^3An)]^{2+*}$ by PQ^{2+} leads to Ru^{III} rather than to An^+. As shown in Scheme III, initial oxidation occurs at ^{3}An but is followed by rapid intramolecular electron transfer from Ru^{II} to $-An^+$ (reaction 2). The intramolecular electron-transfer step leads to formation of Ru^{III} as the final site of oxidation. With the appearance of Ru^{III} as the oxidized site, the spin prohibition to back electron transfer is lost due to spin–orbit coupling. The separation efficiency falls to a value within experimental error of the value found for the $[Ru(dmb)_3]^{2+}/PQ^{2+}$ system.

Scheme III

$$[(bpyCH_2OCH_2An)_2Ru^{II}(bpyCH_2OCH_2{}^3An)]^{2+*} + PQ^{2+} \rightarrow [(bpyCH_2OCH_2An)_2Ru^{II}(bpyCH_2OCH_2An^+)]^{3+}, PQ^+ \quad (1)$$

$$[(bpyCH_2OCH_2An)_2Ru^{II}(bpyCH_2OCH_2An^+)]^{3+}, PQ^+ \rightarrow [(bpyCH_2OCH_2An)_2Ru^{III}(bpyCH_2OCH_2An)]^{3+}, PQ^+ \quad (2)$$

$$[(bpyCH_2OCH_2An)_2Ru^{III}(bpyCH_2OCH_2An)]^{3+}, PQ^+ \rightarrow [(bpyCH_2OCH_2An)_2Ru^{III}(bpyCH_2OCH_2An)]^{3+} + PQ^+ \quad (3a)$$

$$[(bpyCH_2OCH_2An)_2Ru^{III}(bpyCH_2OCH_2An)]^{3+}, PQ^+ \rightarrow [(bpyCH_2OCH_2An)_2Ru^{II}(bpyCH_2OCH_2An)]^{2+}, PQ^{2+} \quad (3b)$$

Intramolecular electron transfer must be more rapid than the rate of separation of $[(bpyCH_2OCH_2An)_2Ru^{II}(bpyCH_2OCH_2An^+)]^{3+}$ and PQ^+ from their association complex (reaction 3a). If it were not, an enhanced separation yield would have been observed for $[Ru(bpyCH_2OCH_2An)_3]^{2+*}$.

The thermodynamic driving force for intramolecular electron transfer can be estimated electrochemically. In cyclic voltammograms of CH_3CN solutions (μ = 0.1 M) containing the anthryl-containing complex, an irreversible, multielectron oxidation wave appears at 1.3 V vs SCE. However, the wave shape is complicated by adsorption. For the complex $[Ru(dmb)_3]^{2+}$, $E_{1/2}$ = 1.12 V vs SCE under the same conditions, which provides a reasonable estimate for the Ru(III/II) couple in $[Ru(bpyCH_2OCH_2An)_3]^{2+}$. Previous electrochemical investigations under comparable conditions have reported $E_{1/2}$ values for the one-electron oxidation of anthracene and its alkylated derivatives that fall in the range 0.9–1.2 V.[41-44] Since the $Ru^{II} \rightarrow An^+$ intramolecular electron transfer is spontaneous, a value at the upper end of this range must be the case for the $-An^{+/0}$ couple in $[Ru(bpyCH_2OCH_2An)_3]^{2+}$. A contribution to the relatively high potential for this couple may come from an electrostatic effect due to the dicationic charge on the complex.

Conclusions

The results presented here demonstrate that our strategy for combining, in a single molecular assembly, the desirable features of visible MLCT light absorption and the extended lifetime of an anthryl triplet has been successful. Excitation at the MLCT chromophore followed by rapid intramolecular energy transfer results in a 14% loss in excited-state energy, but with a gain in lifetime to 6 μs. Further, the bimolecular energy-transfer apparatus has been translated to a single molecule. It continues to function even in a frozen solution where, for example, diffusional quenching of $[Ru(dmb)_3]^{2+*}$ by anthracene could not occur.

The goal of achieving an enhanced separation efficiency following oxidative quenching has not been realized because of a competitive intramolecular electron transfer. It should be possible to overcome this deficiency by turning to asymmetrical complexes of the type $[(4,4'\text{-}(X)_2bpy)_2Ru(bpyCH_2OCH_2An)]^{2+}$, where the X groups are electron withdrawing in character. In these chemically modified complexes, the effect of the electron-withdrawing substituents will be to increase $E_{1/2}$ for the $Ru^{III/II}$ couples.[45-47]

(39) Kober, E. M.; Meyer, T. J. *Inorg. Chem.* **1982**, *21*, 3962; **1984**, *23*, 3877.
(40) Ferguson, J.; Herren, F. *J. Chem. Phys.* **1983**, *76*, 45.
(41) Mann, C. K.; Barnes, K. K. *Electrochemical Reactions in Nonaqueous Systems*; Marcel Dekker: New York, 1970; pp 104–115.
(42) Lund, H. *Acta Chem. Scand.* **1957**, *11*, 1323.
(43) Pysh, E. S.; Yang, N. C. *J. Am. Chem. Soc.* **1963**, *85*, 2124.
(44) Neikam, W. C.; Desmond, M. M. *J. Am. Chem. Soc.* **1964**, *86*, 4811.
(45) Saiji, T.; Aoyagui, L. *J. Electroanal. Chem. Interfacial Electrochem.* **1975**, *60*, 1; **1975**, *58*, 401.

This will prevent intramolecular electron transfer. There will be the additional bonus that the substituent effects will, at the same time, decrease the energy of the lowest lying MLCT states and, therefore, the energy gap between the MLCT and ^{3}An states. As the energy gap is lowered, it will be possible to decrease the extent of excited-state energy lost in the intramolecular energy-transfer event.

Acknowledgments are made to the National Science Foundation under Grant CHE-8806664 for support of this research and to the SERC for postdoctoral support for S.B.

Registry No. $[Ru(bpyCH_2OCH_2An)_3][PF_6]_2$, 122020-09-1; $bpyCH_2OCH_2An$, 122020-07-9; $Ru(dmso)_4Cl_2$, 59091-96-2; 9-anthracenemethanol, 1468-95-7; 4-(bromomethyl)-4′-methylbipyridine, 81998-05-2.

(46) Balzani, V.; Tunis, A.; Barigelletti, F.; Belser, P.; Von Zelewsky, A. *Sci. Pap. Inst. Phys. Chem. Res.* **1984**, *78*, 78.
(47) Barqawi, K. R.; Llobet, A.; Meyer, T. J. *J. Am. Chem. Soc.* **1988**, *110*, 7751.

Directional Electron Transfer: Conformational Interconversions and Their Effects on Observed Electron-Transfer Rate Constants

Bruce S. Brunschwig* and Norman Sutin*

Contribution from the Chemistry Department, Brookhaven National Laboratory, Upton, New York 11973. *Received February 17, 1989*

Abstract: The interaction between conformation changes and electron-transfer rates is considered for systems containing two redox centers. The effect of conformation changes on the free-energy barrier to intramolecular electron transfer is examined. Unstable conformers R* of the reactant (or P* of the product) that are either more (low-λ intermediates) or less (high-λ intermediates) redox-active than the stable reactant R (or product P) are considered. The relative energies of the conformers determine whether the observed electron-transfer reaction proceeds by a two-step mechanism involving the intermediate formation of an unstable conformer or by a direct (concerted) reaction involving only the stable reactant and product. In the normal free energy region, reactions with high-λ intermediates never compete with the direct reaction. The low-λ R* mechanism is favorable only at low driving force when the R* intermediates are just slightly less stable than R, while the P* mechanism can be favorable over the entire free energy region. In the inverted free energy region, reactions involving low-λ P* and high-λ R* or P* intermediates can be more rapid than the direct reaction. Such two-step mechanisms can mask the reduction in rate with increasing driving force expected for the direct reaction in the inverted region. The present analysis generates a set of equations that indicate when the two-step or the direct mechanism is energetically favored. Only when the two-step mechanisms are favored is "gating" or conformational control possible. Reactions with rates that explicitly depend upon the "direction" of electron transfer can still be observed even when gating is absent: because the P* mechanism is favorable over a broader range of free energies and stabilities than the R* mechanism, the overall reaction can have different mechanisms for the forward and reverse directions. Thus conformation changes alone can give rise to directional and/or gated electron transfer.

Intramolecular electron transfer within "supramolecular" systems consisting of several redox components[1-4] or within large molecules, such as native and derivatized metalloproteins,[5-9] are of considerable current interest. Such systems allow the study of the effects of distance and driving force on electron-transfer rates and afford a valuable opportunity for testing theoretical models. While these studies are yielding important information, interpretation of the measured rates requires detailed knowledge of the structures of the reactants and products. In addition, possible conformation changes need to be considered:[7,10] directional and/or "gated" electron transfer may be observed in systems where the stable form of the reactant is redox-inactive but where a less stable, but more redox-active, conformer of the reactant is attainable. Alternatively, for reactions in the inverted region, a mechanism involving a relatively redox-inactive conformer may be favorable!

The question of directional electron transfer has been considered by a number of authors. It has recently been invoked to rationalize an "anomalous" rate of the intramolecular electron transfer between the iron and ruthenium centers in a modified cytochrome *c*.[7] The oxidation of the Fe(II) heme by $Ru^{III}(NH_3)_4$(isn) attached to the histidine-33 residue of cytochrome *c* is much slower[7] than the reduction of the Fe(III) heme by a bound $Ru^{II}(NH_3)_5$ moiety[5] despite the very similar driving forces for the two reactions. Isied and co-workers[7] have interpreted this apparent dependence of the rate on direction by proposing that the iron(II) protein undergoes a conformation change prior to its oxidation to iron(III). Hoffman and Ratner[10] have considered the consequences of coupled conformation and electron-transfer reactions and concluded that, for systems with conformational equilibria, the reaction will *always* proceed by a two-step rather than by a concerted mechanism.[10] In this paper we consider multistep electron-transfer reactions and derive the conditions under which a two-step mechanism will be

(1) Hush, N. S.; Paddon-Row, M. N.; Cotsaris, E.; Oevering, H.; Verhoeven, Z. W.; Heppner, M. *Chem. Phys. Lett.* **1985**, *117*, 8-11.
(2) Isied, S. S.; Vassilian, A.; Magnuson, R. H.; Schwarz, H. A. *J. Am. Chem. Soc.* **1985**, *107*, 7432-7438.
(3) Isied, S. S.; Vassilian, A.; Wishart, J. F.; Creutz, C.; Schwarz, H. A.; Sutin, N. *J. Am. Chem. Soc.* **1988**, *110*, 635-637.
(4) Wasilewski, M. R.; Niemczyk, M. P. *ACS Symp. Ser.* **1986**, *321*, 154-165.
(5) Isied, S. S.; Kuehn, C.; Worosila, G. *J. Am. Chem. Soc.* **1984**, *106*, 1722-1726.
(6) Nocera, B. G.; Winkler, J. R.; Yocom, K. M.; Bordignon, D.; Gray, H. B. *J. Am. Chem. Soc.* **1984**, *106*, 5145-5150.
(7) Bechtold, R.; Kuehn, C.; Lepre, C.; Isied, S. *Nature (London)* **1986**, *322*, 286-288.
(8) Liang, N.; Kang, C. H.; Ho, P. S.; Margoliash, D.; Hoffman, B. M. *J. Am. Chem. Soc.* **1986**, *108*, 4665-4666.
(9) Liang, N.; Pielak, G. J.; Mauk, A. G.; Smith, M.; Hoffman, B. M. *Proc. Natl. Acad. Sci. U.S.A.* **1987**, *84*, 1249-1252.
(10) Hoffman, B. M.; Ratner, M. R. *J. Am. Chem. Soc.* **1987**, *109*, 6237-6243.

0002-7863/89/1511-7454$01.50/0